PERGAMON

International Journal of Solids and Structures 36 (1999) 65–78

INTERNATIONAL JOURNAL OF SOLIDS and STRUCTURES

Investigation of electronic packaging materials by using a 6-axis mini thermo-mechanical tester

Minfu Lu[a], Zhengfang Qian[a], Wei Ren[a], Sheng Liu[a,*], Dongkai Shangguan[b]

[a]*Electronic Packaging Laboratory, Dept. of Mechanical Engineering, Wayne State University, Detroit, MI 48202, U.S.A.*
[b]*Automotive Products Operations, Ford Motor Company, Dearborn, MI 48121-6010, U.S.A.*

Received 4 February 1997; in revised form 12 September 1997

Abstract

Most existing mechanical testers are at most bi-axial and in general too large for microelectronic materials and structures. Existing mini testers are primarily single axis without any active specimen alignment monitoring and adjustment capability. Fundamental investigation needs to be conducted for packaging materials in terms of deformation and fracture processes, constitutive laws, and failure quantities. In this paper, a unique 6-axis sub-micron thermo-mechanical fatigue tester is described, including some calibration work for both load cell and machine stiffness. For the first time, an active specimen alignment monitoring and adjustment was demonstrated on a single lap shear sample, assisted by a high resolution laser moiré measurement system. This paper also presents results for two types of polymer films, one lead-free solder alloy, and some other conventional materials. In particular, deformation and failure mechanisms for two polymer films have been discussed.

1. Introduction

The reliability of high performance packaging is closely governed by the thermo-mechanical properties of its constituent materials, interconnects, their interfaces, and their microstructures (Liu et al., 1995). For instance, polyimide films are widely used as passivation coatings on the silicon chip surface, and dielectric layers in high density interconnects (HDI) due to their excellent electrical properties. Their properties are known to be temperature, time, and thickness (scale) dependent. Their interfaces to other materials are critical to the reliability of next generation low cost flip-chip packages. However, it is very challenging to obtain reliable, consistent, comprehensive material data for the purpose of mechanical design, reliability assessment and process optimization. For instance, specimen alignment of micro-solids or brittle materials such as silicon and ceramic, an usually ignored issue, can be important during the testing. Large errors can be generated for

* Corresponding author. Tel.: 001 313 577 3843; fax: 001 313 577 8789; e-mail: sliu@eng.wayne.edu

PII: S0020-7683(97)00281-3

small brittle specimens without proper alignment and in some instances specimens can be easily damaged. Currently, a few in-house single axis testers exist in some universities and industrial laboratories. Testers driven by piezoelectric stacks in general have a small travel range of micrometers. Stepper motor driven testers can have large travel range but may generate non-smooth load displacement curves due to their open loop control. Electromagnetic coil driven testers may have over-heating problems. With the rapid advances made in DC motors integrated with encoder based displacement closed loop control, sub-micron resolution can be achieved (Newport Catalog, 1996). In addition, one common drawback of the existing single axis testers is that they do not have an active alignment monitoring and adjustment system. This issue could be critical for brittle materials, miniaturized samples, such as those in electronic packaging, micro sensors/actuators, MEMS (microelectronical and mechanical systems), precious metal testing, and other micromechanical testing. For instance, it is difficult to grip a silicon chip without monitoring the clamping induced moments and forces. Therefore, it is difficult to control failure process consistently that raises some doubts on the reliability of the material data because those testers do not have the capability for specimen alignment. An active alignment monitoring and adjustment is therefore essential for reliable material testing so that fundamental understanding of material and structural behaviors can be obtained.

Due to many fabrication steps involved in manufacturing microelectronic devices, thermal cycling and thermal shock are involved in addition to mechanical loading. Due to the mismatch in thermo-mechanical properties of materials involved, the materials and the device are likely subjected to multi-axial stress state. It would be desirable to have a testing machine that can be used for both material and structural testing such that multiple loads can be applied in various combinations, similar to a multi-degree of freedom manipulator. For instance, the mode mixity of an interfacial crack tip could be controlled by choosing certain loading sequence or simultaneous loading without using a complex fixture.

A 6-axis sub-micron tester, recently designed and built at Wayne State University (Lu et al., 1996), is a general purpose micromechanical/thermal fatigue testing instrument, fully controlled by a PC computer. The machine can apply displacements/loads to the tested specimen along six degrees of freedom, i.e., three orthogonal translations and three rotations. The displacement resolutions of each closed-loop, DC-motor-drive stage is maintained at 0.1 μm in translations and 0.001 degree in rotations (Newport Catalog, 1996). Machine stiffness calibration was reported in (Lu et al., 1996a) and some results will also be presented in the coming section. For quasi-static and low frequency applications, or those applications with large deformation, translational displacement readings directly out of the DC motor travel distance subtracting the elastic deformation of the stage can be used with good confidence. In general, a capacitance gage or a linear encoder is used to measure the actual displacement of a test sample. For rotational displacements, direct motor position subtracting the torsional stiffness of the stage induced displacement is currently used. Due to the precision of both linear encoders and rotary encoders and closed loop control integrated in the DC motors, linearity can be maintained to be less than 0.1% and the resolution achieved can provide accurate measurements for small samples.

Due to the harsh thermal environment for automobile electronic devices and many others, material behaviors at high and low temperatures are needed for both material evaluation and performance prediction. This tester is suitable for the study of the behaviors of packaging structures and their materials at the temperature ranging from -128°C to 600°C. The integrated high

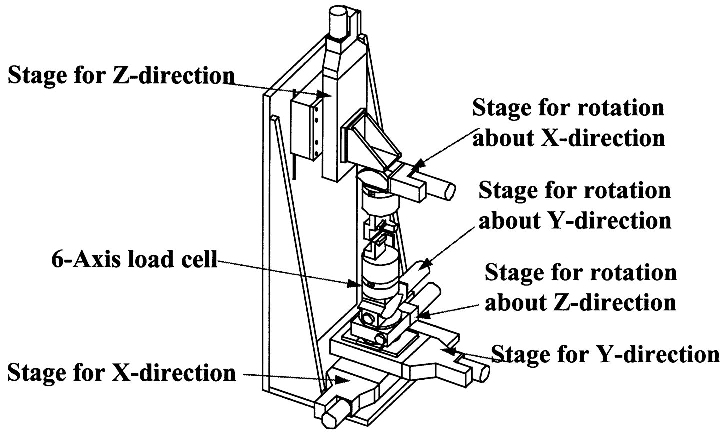

Fig. 1. Vertical orientation of the tester.

temperature/cryogenic multi-grip set is connected to a 6-axis load cell and the stages to perform up to six axes of tests. A small environmental chamber is capable of surrounding the grips that allows testing at a ramping temperature to extreme hot and cold points. Due to the temperature sensing and the closed loop, stable temperature can be achieved with 1°C maximum variation, even for creep testing. An optical image processing system is used on a TV monitor to help mount very small samples or observe the deformation of the sample during loading. The machine can operate in two orientations: vertical for long specimens and three-point or four-point bending, horizontal when the temperature chamber is used. Figures 1 and 2 show some typical configurations of the mini-tester.

2. Calibration of the machine

The machine is calibrated in two steps. First, the 6-axis load cell is calibrated by adding some deadweights. A specially designed apparatus with holes on its four ends is fixed on the top of the load cell for calibration purposes as shown Fig. 3. More complete results of the calibrated load cell were presented in (Lu et al., 1996b). The calibration for the movement of stages was implemented by employing a laser measurement system.

Due to the rather large compliance of the stages used in the machine, machine stiffness measurement for all six stages must be performed before any actual test can be conducted. A rigid block is fixed at the two grips as shown in Fig. 4. By applying a certain movement of the stage, a loading-displacement curve is recorded. It is assumed that the rigid block's stiffness is so large that there is no displacement between the two grips. The measured displacement of the stage is primarily caused by the deformation of the stages and other fixtures of the machine. Figure 5 shows a loading-displacement curve in Z direction. The slope of the curve is the machine stiffness in that direction. The stiffness of that direction is 106,375 g/mm. After the machine stiffness matrix is obtained, the actual displacement for each direction can be modified as follows:

$$d_j(i) = D_j(i) - F_j(i)/E_j, \quad i = 1,2,\ldots,6$$

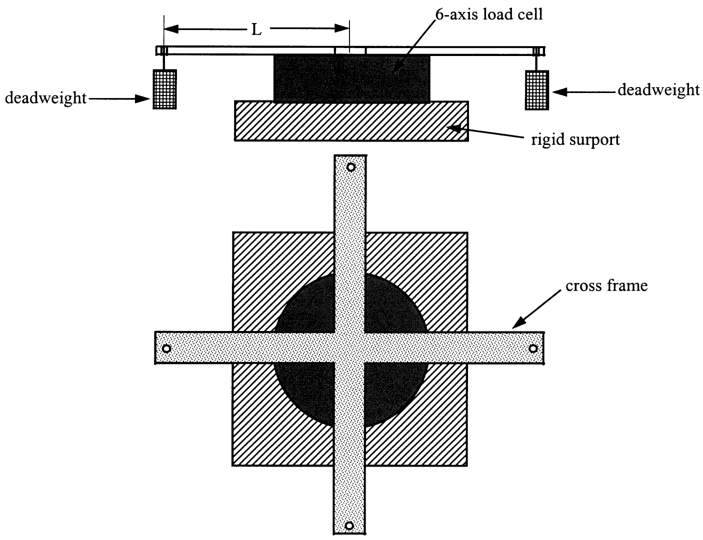

Fig. 3. Calibration apparatus for the 6-axis load cell.

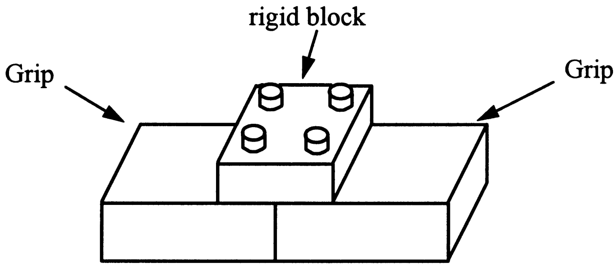

Fig. 4. Schematic drawing of a rigid block mounted at the two grips.

were d_j is the modified displacement, D_j is the measured movement of j-th stage, F is load, and E_j is the machine stiffness in the jth direction. Several common engineering materials have been tested for their Young's modulus and the results agreed with the literature (Lu et al., 1996a). However, these results are not described in this paper. These materials include an aluminum strip (0.48 mm × 3.87 mm × 3.18 mm), a pure copper wire of diameter 0.8 mm and a stainless steel foil of thickness 50 μm.

3. Applications

3.1. *Specimen alignment monitoring and adjustment during test*

Silicon/solder/copper layered system is a typical packaging sub-assembly as copper is a good heat sink material which can rapidly dissipate heat induced by silicon chip heating. Single lap shear

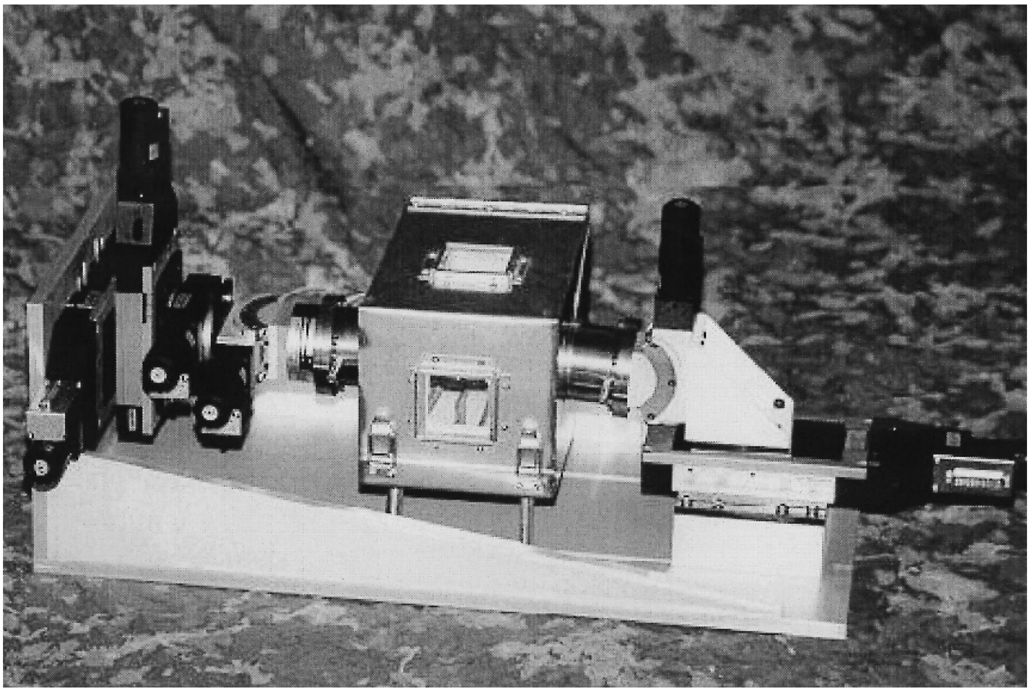

Fig. 2. Horizontal orientation with an environmental chamber.

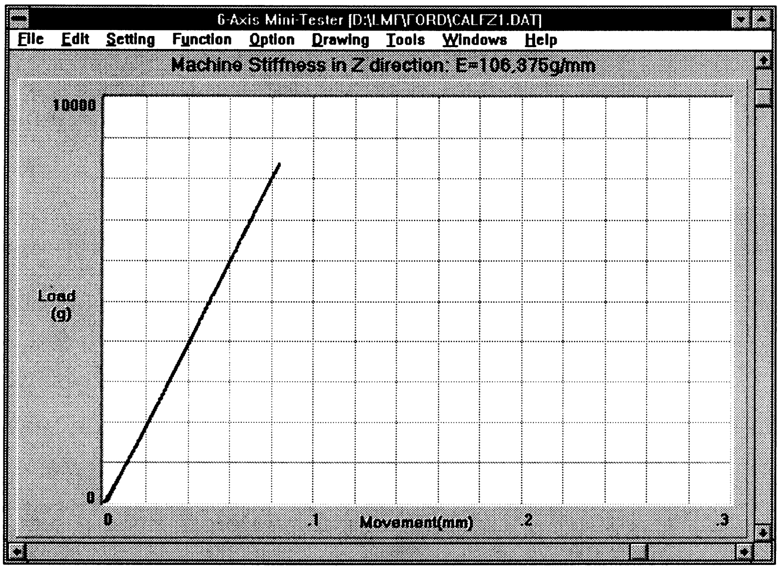

Fig. 5. Load-displacement curve of the machine stiffness measurement.

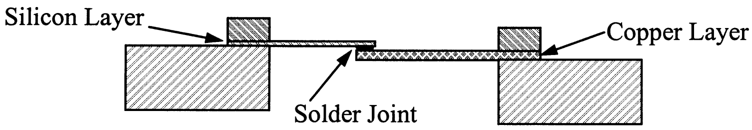

Fig. 6. Schematic drawing of a silicon-copper single lap sample.

joint specimens are widely used for both the adhesion testing and engineering shear testing. However, it is a challenge to grip brittle materials or structures to obtain their mechanical behavior. For example, when a silicon-copper single lap sample is gripped for a tensile test as shown in Fig. 6, it is very difficult to perform a test in tension without introducing bending moments and other undesirable forces and moments. Unfortunately, even a small bending moment could cause a brittle material to break. However, by monitoring all 6-axis forces and moments, and releasing any unnecessary mounting forces by micropositioning the corresponding stages during or after mounting the sample, those undesirable forces/moments can be reduced to zero.

Another aspect of misalignment is that it can introduce large error to final results. When a copper single lap specimen is mounted to the mini tester, a large preloaded compression force can be introduced to the specimen due to the deformation of the copper caused by the compression force of the clamps. The preloaded forces are shown schematically in Fig. 7. During mounting, a high resolution, non-contact and real time interferometry moiré technique (Post et al., 1993) is introduced to monitor the deformation of the sample. The fringe patterns are shown in Fig. 8. Fig. 9 shows a graphic-user-interface monitoring the forces induced during the mounting process. Experimental results show that the error in final failure load caused by preloading can be as large as 25% without proper alignment.

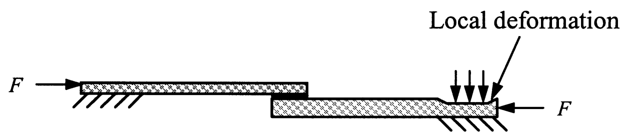

Fig. 7. Schematic drawing of preloaded forces.

(a)

(b)

Fig. 8. Fringe patterns without alignment (left) and with alignment (right).

3.2. *A lead-free solder alloy joint in shear*

Lead-tin alloys such as 63Sn/37Pb and 62Sn/36Pb/2Ag (by weight) are currently the prevalent materials used to attach electronic components onto the electronic circuitry on the substrate. Due to the increasing environmental concern, careful considerations have been given to the eutectic Sn-Ag (96.5%Sn-3.5%Ag by weight). This material has melting temperature of 221°C and coefficient of thermal expansion (CTE) of 22 ppm/C. Material tensile properties as a function of temperature and strain rates that are obtained will be reported in a later article and the effort in this paper is focused on the nominal shear strength obtained on single lap shear specimens (Shangguan and Achari, 1995, Shangguan et al., 1994).

In order to obtain the average shear strength of this new lead-free solder alloy, which is a potential candidate for future solder joint materials in automobile electronic packaging industry (Shangguan and Achari, 1995). Several samples were fabricated in an oven and naturally cooled to the room temperature for a controlled microstructure. Due to the outgassing of flux during the wave soldering process, voids cannot be avoided in sandwiched specimens. The larger the sample

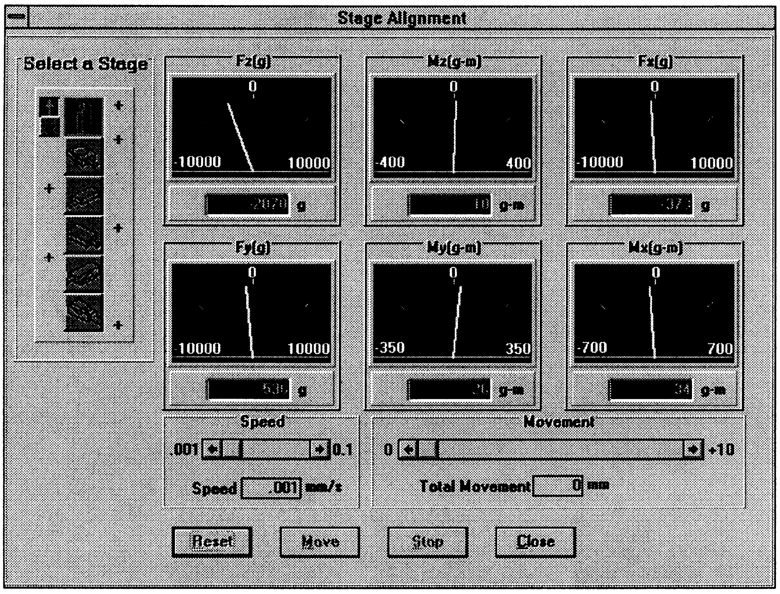

Fig. 9. Graphic user-friendly interface for monitoring preload forces.

is, the more voids are present. The voiding area is measured by examining the failed samples by an imaging processing scheme. For instance, for a specimen with 250 mm^2 shearing area solder layer, the voiding volume ratio could be more than 30%. In contrast, a small sized specimen with 2 mm^2 testing area, the void can be less than 5%. Several small sized lead-free solder alloy sandwiched specimens are tested at the 6-axis test machine. One of loading-displacement curves is shown in Fig. 10. Significant nonlinear behavior was observed and the delamination initiation was found to occur along the cooper/solder interface, followed by an unstable crack growth before the collapse of the joint. The shear strength of the new material is 34.24 MPa. Testing was also conducted for a eutectic solder alloy (63Sn/37Pb) and the obtained shear strength is from 39 MPa to 40 MPa. It is noted that the applied deformation rate is 0.005 mm/s

3.3. *Thin films*

Two types of polymer thin films have been tested on the mini-tester. The first is a polycarbonate film provided by a Japanese vendor. The second is Kapton® of DuPont, which is made from pyromellitic dianhydride (PMDA) and 4–4″ oxydianilline (ODA). The chemical structure of the Kapton can be found in (Pecht and Wu, 1994). All film specimen sizes are 6.0 mm $\times$ 22 mm as recommended by ASTM standard D882-88. The thickness of polycarbonate specimen is 50 μm and the thicknesses of Kapton specimens are 25, 40 and 150 μm. Strain rate for Kapton films used to compare the thickness effect is 9.1E-3/s recommended by ASTM standard D882-88. Creep tests were performed on a polycarbonate strip (0.05 mm $\times$ 6 mm $\times$ 20 mm) with holding force of 1300 grams. Loading and unloading test is also conducted for a polycarbonate strip (0.05 mm $\times$ 6 mm $\times$ 20 mm)

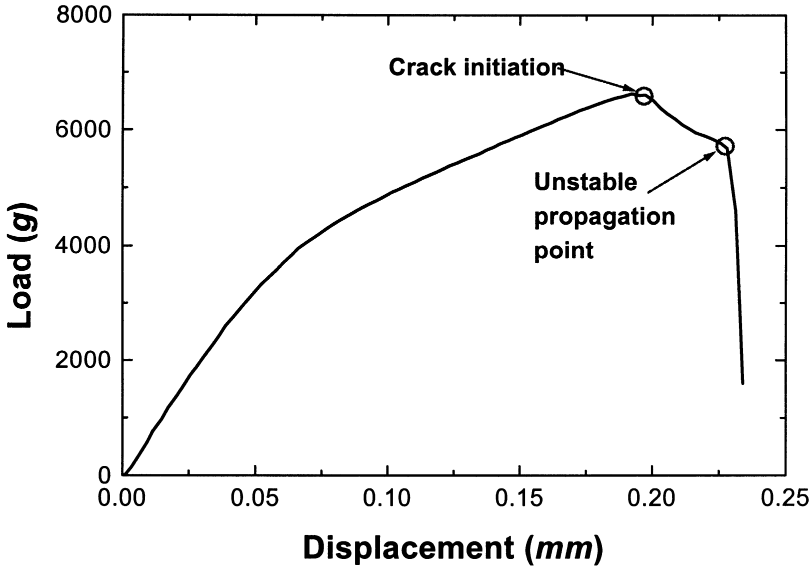

Fig. 10. Loading-displacement curve of a lead-free solder alloy specimen.

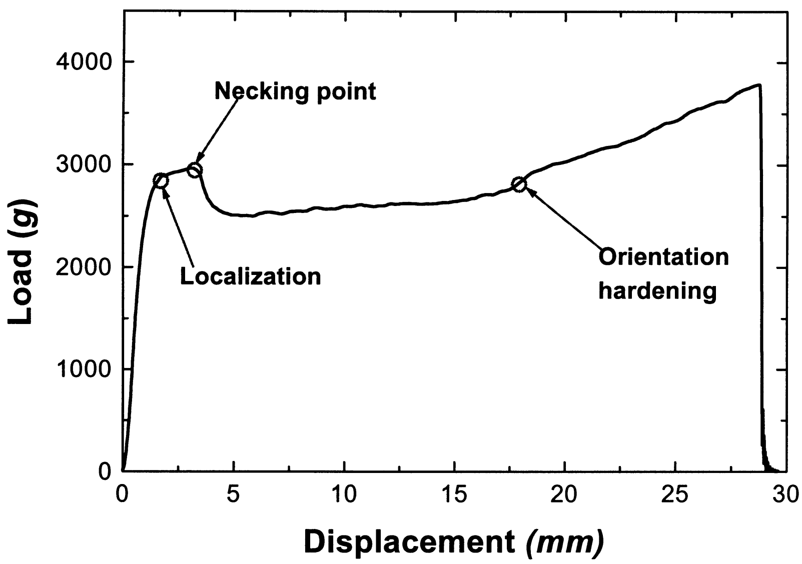

Fig. 11. Loading curve of a polycarbonate strip (thickness = 0.05 mm).

Appropriate efforts were made to prevent the sliding and ensure failure occurs at the center section instead at clamped edges. A typical load-displacement for a polycarbonate film is shown in Fig. 11, demonstrating a very nonlinear behavior showing the sequence of localization, necking,

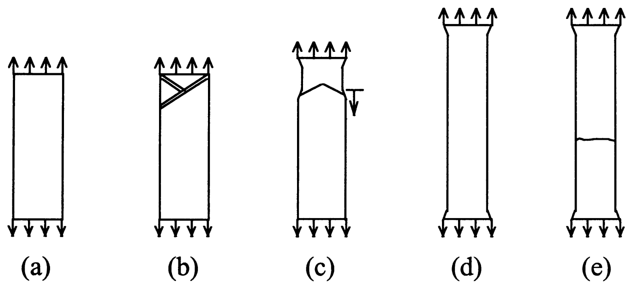

Fig. 12. Mechanisms of deformation and failure of polycarbonate. (a) before necking, (b) localization initiation, (c) necking propagation, (d) orientational hardening, (e) rupture.

necking propagation, and molecular orientation hardening. Figure 12 schematically demonstrates the mechanisms of the deformation and failure of the polycarbonate film. Figure 13 shows the true stress-strain curves of polycarbonate strips under three different rates, indicating the rate dependent behavior. It is also shown in Fig. 13 that much longer steady necking propagation and much stronger orientation hardening are observed for films than those of bulk polycarbonate (Boyce et al., 1994). Difference in manufacturing techniques for making both the thin films and the bulk polycarbonate materials may contribute to this phenomenon. However, the molecular chains for thin films are constrained mainly in the plane of the thin films so that the orientation hardening should be much larger than the bulk materials. This reasoning is also supported by the thickness effect of Kapton films available for this study, as shown in Fig. 14. It is clear that the thinner the film more significant the hardening. This fact also shows that it is important to obtain realistic properties of films to propose analytical models for the design of electronic packaging materials and structures. Temperature dependent behavior of the polycarbonate film is also shown in Fig. 15. A creep curve of a polycarbonate stripe sample at 1300 grams loading is shown in Fig. 16.

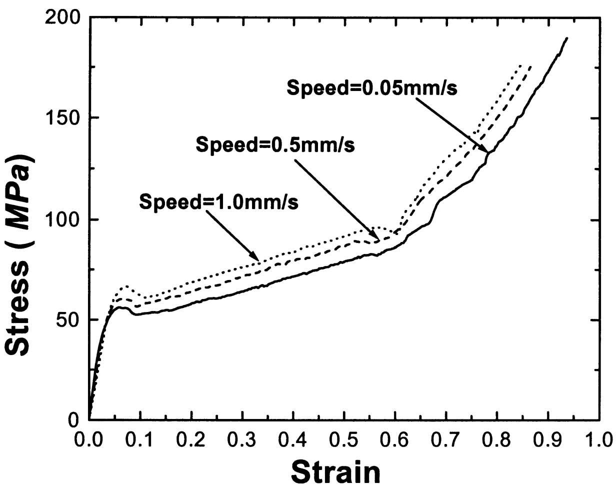

Fig. 13. True stress-strain curves of polycarbonate strips under three different loading rates.

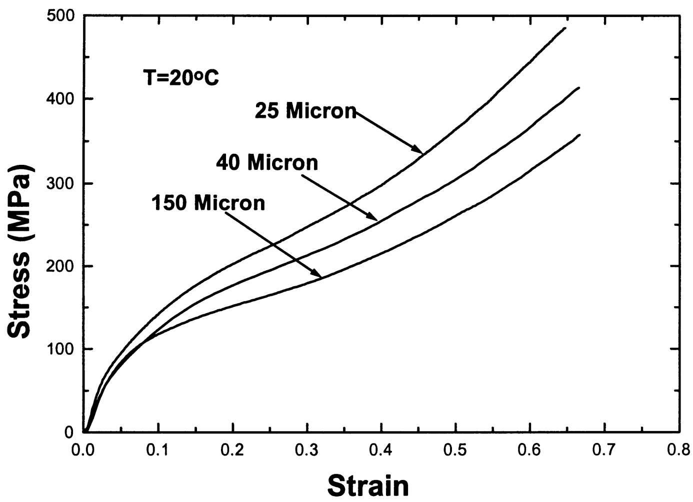

Fig. 14. Thickness effect of Kapton®ployimide film.

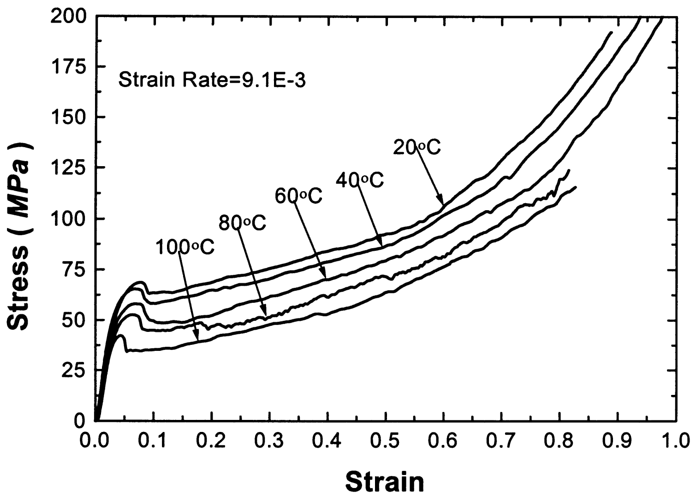

Fig. 15. Temperature dependent behavior of polycarbonate film.

Finally, a loading and unloading curve of a polycarbonate strip is also presented. Significant nonlinear behavior has been observed. Further analytical work on polymer films will be reported in a subsequent paper.

4. Conclusions

The mechanical behavior of several electronic packaging materials is investigated by using a thermo-mechanical mini-tester developed at Wayne State University. Experimental results have

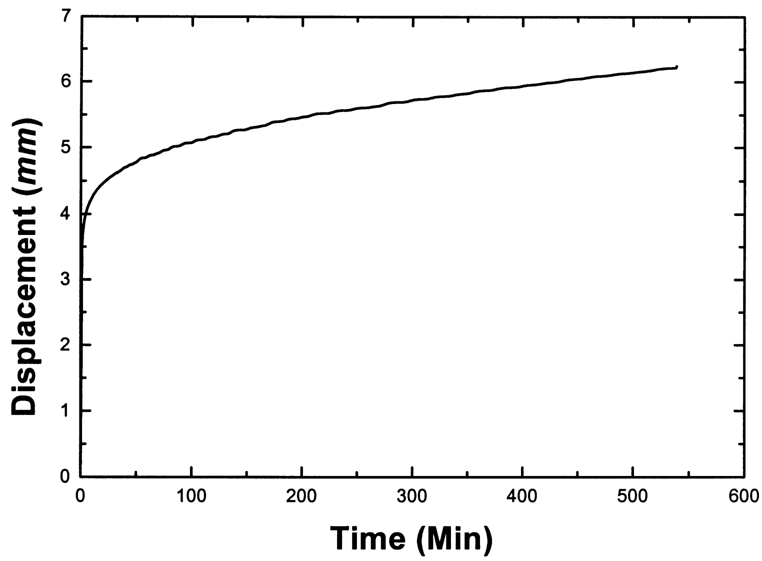

Fig. 16. Creep curve of a polycarbonate stripe sample at a 1300 grams load.

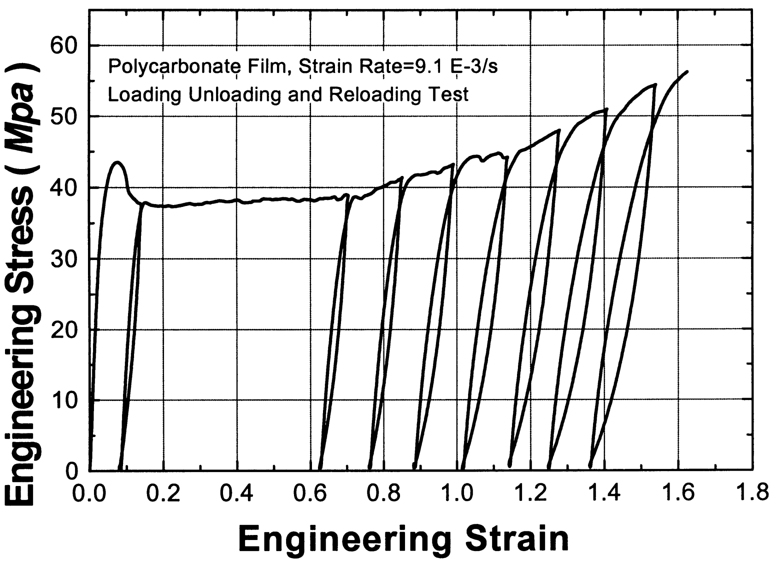

Fig. 17. Loading and unloading behavior of a polycarbonate strip.

demonstrated that the machine is suitable for investigating the behavior of small specimens, particularly, in the field of electronic packaging. Active specimen alignment monitoring and adjustment has been demonstrated to be important for small samples. Failure mechanisms observed have been explained.

Acknowledgments

The authors would like to acknowledge the support from NSF Presidential Faculty Fellows Award, NSF U.S.-Japan Cooperative Research, the Ford Motor Company, and Semiconductor Research Cooperation. The authors also appreciate the help from Prof. Kishimoto of Tokyo Inst. of Technology for providing the polycarbonate films, and Dr C. P. Yeh and Dr S. Wu of Motorola for providing the Kapton films. Finally, the constructive comments from two reviewers are also gratefully acknowledged.

References

Boyce, M.C., Ellen, M.A., Jayachandran, R., 1994. The large strain compression, tension, and simple shear of polycarbonate. Poly. Eng. Sci., 34, 716–725.
Liu, S., Zhu, J., Hu, J.M., Pao, Y.H., 1995. Investigation of crack propagation in ceramic/adhesive/glass systems, IEEE Trans., CHMT, Sept.
Lu, M., Ren, W., Liu, S.A., 1996. Multi-axial thermo-mechanical fatigue tester for electronic packaging materials. ASME Symposium of Sensoring, Monitoring, Modeling and Verification of Electronic Packaging, Nov. 17–21, Atlanta, pp. 87–92.
Lu, M., Ren, W., Liu, S.A., 1996. Unique multi-axial thermo-mechanical fatigue tester for electronic packaging materials. The Second International Symposium on Electronic Packaging Technology. Shanghai, Dec. 9–12, China.
The Newport Catalog, 96/97, Newport Corporation, 1996.
Pecht, M., Wu, X., 1994. Characterization of polyimides used in high density interconnects. IEEE Transaction on Components and Manufacturing Technology-Part B, 17(4).
Post, D., Han, H., Ifju, P., 1993. High Sensitive Moiré: Experiment Analysis for Mechanics and Materials, Springer-Verlag, NY.
Shangguan, D., Achari, A., 1995. Lead-free solder alloys, U.S. Patent No. 5,429,689.
Shangguan, D., Achari, A., Green, W., 1994. Application of lead-free eutechnic Sn-Ag solder in no-clean thick film electronic modules. IEEE Transactions CPMT—Part B, 17(4), 603–611.